Available online at www.sciencedirect.com
SCIENCE DIRECT®
PERGAMON
Polyhedron 22 (2003) 2311–2315
POLYHEDRON
www.elsevier.com/locate/poly

Crystal structures and magnetic properties of (m- or p-MPYNN)$_2$ Ni^{II}(tdas)$_2$

Tsunehisa Okuno [a,*], Kazunori Kuwamoto [a], Wataru Fujita [b], Kunio Awaga [b], Warô Nakanishi [a]

[a] Department of Material Science and Chemistry, Faculty of Systems Engineering, Sakaedani, Wakayama 640-8510, Japan
[b] Department of Chemistry, Graduate School of Science, Nagoya University, Chikusa, Nagoya 464-8602, Japan

Received 7 October 2002; accepted 31 January 2003

Abstract

Novel Ni^{II}(tdas)$_2$ complexes, (m- or p-MPYNN)$_2$Ni(tdas)$_2$ (MPYNN = N-methylpyridinium α-nitronyl nitroxide and tdas = 1,2,5-thiadiazole-3,4-dithiolate), were prepared. The Ni(tdas)$_2$ anions are located on the lattice points and at the lattice center in the crystal of (m-MPYNN)$_2$Ni(tdas)$_2$. The m-MPYNN cations form a centrosymmetric dimer, and the anion is sandwiched by a pair of the dimers, forming alternate stacks along the a axis. In the crystal of the (p-MPYNN)$_2$Ni(tdas)$_2$ complex, the Ni(tdas)$_2$ anions are located on the lattice points and at the center of the bc plane. The anion is surrounded by four p-MPYNN cations. The p-MPYNN cations also form a centrosymmetric dimer. Each cation has a short contact with a different Ni(tdas)$_2$ anion. The magnetic susceptibilities of both complexes decrease with decreasing temperature, indicating antiferromagnetic interaction within the radicals. The behavior of (m- and p-MPYNN)$_2$Ni(tdas)$_2$ was understood with the singlet–triplet model and the Curie–Weiss law.
© 2003 Elsevier Science Ltd. All rights reserved.

Keywords: Centrosymmetric dimer; Antiferromagnetic interaction; Singlet–triplet; Curie–Weiss law

1. Introduction

Growing interest has been paid to molecular magnets with high electrical conductivity [1]. One of the strategies for the construction of an organic magnetic metal is hybridization with a conducting backbone and magnetic moments, which are weakly coupled with each other.

Awaga et al. prepared N-alkylated PYNN radicals [2,3], where PYNN = pyridyl α-nitronyl nitroxide. One of the characteristics of the radical family is to have a positive charge on the pyridyl ring, which makes it possible to introduce several compounds as a counter anion system [4]. In the case of the salt of the Ni^{III}(dmit)$_2$ anion, the obtained salt, (p-EtPYNN)Ni(dmit)$_2$, showed a particularly interesting magnetic behavior which was explained by the spin-ladder model [5].

The Ni(tdas)$_2$ anion [6–8], where tdas = 1,2,5-thiadiazole-3,4-dithiolate, has also given conducting materials similarly to Ni(dmit)$_2$, such as (TTF)$_2$Ni(tdas)$_2$ [9]. Although the conductivity is low, (OMTTF)$_2$Ni(tdas)$_2$ (OMTTF = octamethylene-tetrathiafulvalene) was also reported [10]. One of the most notable differences between Ni(tdas)$_2$ and Ni(dmit)$_2$ is the pattern of the spatial contact. The Ni(tdas)$_2$ molecule is expected to have strong intermolecular contact at the –NSN– moieties. Although the M(tdas)$_2$ (M = Ni, Pd, Pt, Cu and Fe) anions also have a high possibility of forming a variety of metal–organic complexes, only a few studies concerning the compounds were reported [9–11].

In this paper, we report the crystal structures and the physical properties of the novel Ni^{II}(tdas)$_2$ complexes, where the m- or p-MPYNN (MPYNN = N-methylpyridinium α-nitronyl nitroxide) radicals are introduced as counter cations (Fig. 1).

* Corresponding author. Tel.: +81-73-457-8264; fax: +81-73-457-8264.
E-mail address: okuno@sys.wakayama-u.ac.jp (T. Okuno).

0277-5387/03/$ - see front matter © 2003 Elsevier Science Ltd. All rights reserved.
doi:10.1016/S0277-5387(03)00214-6

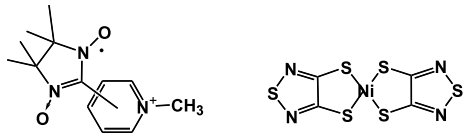

m- or *p*- MPYNN Ni(tdas)$_2$

Fig. 1. Chemical structures of the *m*- or *p*-MPYNN cation and the Ni(tdas)$_2$ anion.

2. Experimental

2.1. General procedures

Infrared spectra were recorded on a JASCO FT/IR-420 spectrometer with samples in compressed KBr discs. $TEA_2Ni(tdas)_2$ (TEA = tetraethylammonium) and *m*- or *p*-MPYNNI (*m*- or *p*-MPYNNI = [3- or 4-(4,4,5,5-tetramethyl-1-oxido-3-oxyl-4,5-dihydro-3*H*-imidazol-2′-yl)-1-methylpyridinium] iodide) were prepared according to procedures in the literatures [2,3,6,7].

2.2. (*m*-MPYNN)$_2$Ni(tdas)$_2$

$TEA_2Ni(tdas)_2$ (185 mg, 0.30 mmol) and *m*-MPYNNI (240 mg 0.61 mmol) were dissolved in acetonitrile (20 ml). The solution was refluxed for 10 min and then filtered. The filtrate was placed in a refrigerator overnight, and the black crystals were isolated by filtration.

(*m*-MPYNN)$_2$Ni(tdas)$_2$ (120 mg, 47%): black needles, m.p. 124 °C (dec.), Found: C, 42.18; H, 4.49; N, 16.26. Calc. for $C_{30}H_{38}N_{10}O_4S_6Ni_1$: C, 42.20; H, 4.49; N, 16.41%. IR: 1523 w, 1453 w, 1376 m, 1320 s, 1229 s, 1139 w, 768 m, 666 m.

2.3. (*p*-MPYNN)$_2$Ni(tdas)$_2$

The *para* complex was prepared by the same method from $TEA_2Ni(tdas)_2$ and *p*-MPYNNI. The yield was 27%: black needles, m.p. 130 °C (dec.), Found: C, 42.38; H, 4.52; N, 16.51. Calc. for $C_{30}H_{38}N_{10}O_4S_6Ni_1$: C, 42.20; H, 4.49; N, 16.41%. IR: 1641 m, 1560 w, 1526 m, 1442 m, 1416 m, 1372 m, 1318 s, 1231 s, 1197 w, 1168 w, 1144 w, 1023 w, 840 w, 827 m, 785 w, 771 s, 609 m.

2.4. Crystal structure determination of (*m*-MPYNN)$_2$Ni(tdas)$_2$ and (*p*-MPYNN)$_2$Ni(tdas)$_2$

In each case, the crystals were grown by the slow cooling of acetonitrile solutions. Samples were mounted on glassy capillaries. Data collections were performed on a Rigaku AFC 5R, an automatic four-circle diffractometer, at room temperature. The conditions used for crystallographic data collection and structure refinement are summarized in Table 1. Structures were solved by heavy-atom Patterson methods and expanded using the Fourier technique. The non-hydrogen atoms were refined anisotropically. Hydrogen atoms were included but not refined.

Table 1
Crystal data and structure refinement for (*m*-MPYNN)$_2$Ni(tdas)$_2$ and (*p*-MPYNN)$_2$Ni(tdas)$_2$N

	(*m*-MPYNN)$_2$-Ni(tdas)$_2$	(*p*-MPYNN)$_2$-Ni(tdas)$_2$
Formula	$C_{30}H_{38}N_{10}O_4S_6Ni_1$	$C_{30}H_{38}N_{10}O_4S_6Ni_1$
Crystal system	monoclinic	monoclinic
Space group	$P2_1/n$	$P2_1/c$
Crystal color, habit	black, needle	black, needle
a (Å)	7.085(4)	13.010(3)
b (Å)	31.847(5)	10.743(5)
c (Å)	8.686(4)	14.726(3)
α (°)	90	90
β (°)	105.98(4)	114.78(1)
γ (°)	90	90
V (Å^3)	1884(1)	1868.1(10)
Z	2	2
Crystal dimensions (mm)	0.6 × 0.1 × 0.1	0.4 × 0.2 × 0.2
No. data collected	4083	5108
No. unique data	3749	4885
No. observed data ($I > 3\sigma(I)$)	3662	1648
No. variables	233	232
R	0.060	0.048
Rw	0.068	0.034
Goodness of fit	1.33	1.56

2.5. Magnetic measurements

Magnetic susceptibilities were measured on a Quantum Design MPMS-XL SQUID meter in the temperature range of 2–300 K with the external field being 1 T.

3. Results and discussion

3.1. Crystal structure of (*m*-MPYNN)$_2$Ni(tdas)$_2$

The (*m*-MPYNN)$_2$Ni(tdas)$_2$ complex was crystallized in the $P2_1/n$ space group with $a = 7.085(4)$ Å, $b = 31.847(5)$ Å, $c = 8.686(4)$ Å, $\beta = 105.98(4)°$, $Z = 2$. Half of the Ni(tdas)$_2$ anion and that of the *m*-MPYNN cation are crystallographically independent. Fig. 2 shows the molecular structure of (*m*-MPYNN)$_2$Ni(tdas)$_2$. The selected bond lengths and angles are summarized in Table 2. A significant difference cannot be found in the structures of both *m*-MPYNN and Ni(tdas)$_2$, compared with those of the reported ones [3,7]. The dihedral angle between the imidazolyl ring and the pyridyl one is approximately 10°, which is slightly smaller than the reported value.

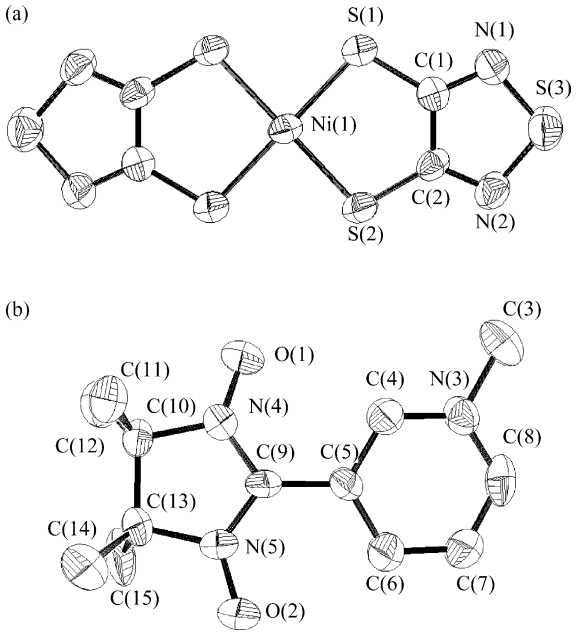

Fig. 2. The molecular structure of the $(m\text{-MPYNN})_2Ni(tdas)_2$ complexes. (a) The $Ni(tdas)_2$ anion; (b) the m-MPYNN cation.

Table 2
Selected bond lengths (Å) and angles (°) for (m- and p-MPYNN)$_2$Ni(tdas)$_2$

$(m\text{-MPYNN})_2Ni(tdas)_2$		$(p\text{-MPYNN})_2Ni(tdas)_2$	
$[Ni(tdas)_2]^{2-}$		$[Ni(tdas)_2]^{2-}$	
Ni(1)–S(1)	2.196(2)	Ni(1)–S(1)	2.208(2)
Ni(1)–S(2)	2.189(2)	Ni(1)–S(2)	2.190(2)
S(1)–C(1)	1.722(6)	S(1)–C(1)	1.743(6)
S(2)–C(2)	1.731(6)	S(2)–C(2)	1.740(5)
S(3)–N(1)	1.661(5)	S(3)–N(1)	1.654(5)
S(3)–N(2)	1.650(5)	S(3)–N(2)	1.648(5)
N(1)–C(1)	1.317(6)	N(1)–C(1)	1.316(6)
N(2)–C(2)	1.327(6)	N(2)–C(2)	1.317(6)
C(1)–C(2)	1.433(7)	C(1)–C(2)	1.430(7)
S(1)–Ni(1)–S(2)	93.14(6)	S(1)–Ni(1)–S(2)	93.48(6)
Ni(1)–S(1)–C(1)	103.1(2)	Ni(1)–S(1)–C(1)	102.1(2)
Ni(1)–S(2)–C(2)	102.7(2)	Ni(1)–S(2)–C(2)	102.9(2)
N(1)–S(3)–N(2)	98.6(3)	N(1)–S(3)–N(2)	98.6(2)
m-MPYNN		p-MPYNN	
N(3)–C(3)	1.472(7)	N(3)–C(3)	1.481(6)
O(1)–N(4)	1.269(5)	O(1)–N(4)	1.267(5)
O(2)–N(5)	1.278(5)	O(2)–N(5)	1.260(6)
N(4)–C(9)–N(5)	108.5(6)	N(4)–C(9)–N(5)	108.9(5)
N(4)–C(9)–C(5)–C(4)	10(1)	N(4)–C(9)–C(6)–C(5)	4.5(9)

Fig. 3 shows the crystal structure of (m-MPYNN)$_2$Ni(tdas)$_2$. The $Ni(tdas)_2$ anions are located on the lattice points and at the center of the unit cell (Fig. 3(a)). The spatial contact between $Ni(tdas)_2$ anions is not recognized. The m-MPYNN molecules are present as a centrosymmetric dimer (Fig. 3(b)). Intradimer contact is observed between the oxygen atom of the

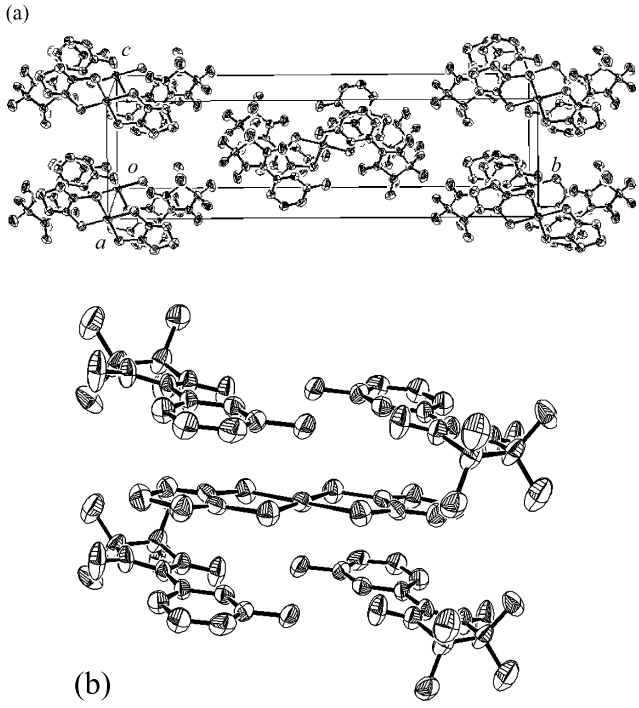

Fig. 3. The crystal structure of $(m\text{-MPYNN})_2Ni(tdas)_2$ (a) the unit cell; (b) the crystal packing around the $Ni(tdas)_2$ anion.

NO group, O(1) and the carbon atom of the N-methyl group, C(3), with the distance being 2.94(1) Å. However, spatial contact between the NO groups is not recognized. The dimer and the $Ni(tdas)_2$ anion form alternate stacks along the a axis. Thus, the $Ni(tdas)_2$ anion is surrounded by four m-MPYNN molecules. The shortest contact between $Ni(tdas)_2$ and m-MPYNN is 3.33(1)Å for C(1)···O(1) (Fig. 3(b)).

3.2. Crystal structure of $(p\text{-MPYNN})_2Ni(tdas)_2$

The $(p\text{-MPYNN})_2Ni(tdas)_2$ complex was crystallized in the $P2_1/c$ space group with $a = 13.010(3)$ Å, $b = 10.743(5)$ Å, $c = 14.726(3)$ Å, $\beta = 114.78(1)^\circ$, $Z = 2$. Half of the $Ni(tdas)_2$ anion and that of the p-MPYNN cation are crystallographically independent. Fig. 4 shows the crystal structure of $(p\text{-MPYNN})_2Ni(tdas)_2$. The selected bond lengths and angles are also summarized in Table 2. The molecular structure of $Ni(tdas)_2$ is omitted, because the anion shows almost the same structure as that mentioned for $(m\text{-MPYNN})_2Ni(tdas)_2$. A significant difference also cannot be found in the structure of p-MPYNN from the reported one. The dihedral angle between the imidazolyl ring and the pyridyl one of p-MPYNN is approximately 5° (Fig. 4(a)).

The $Ni(tdas)_2$ anions are located on the lattice points and at the center of the bc plane (Fig. 4(b)). The $Ni(tdas)_2$ anions form a one-dimensional array along the a axis. The intermolecular distance between the terminal

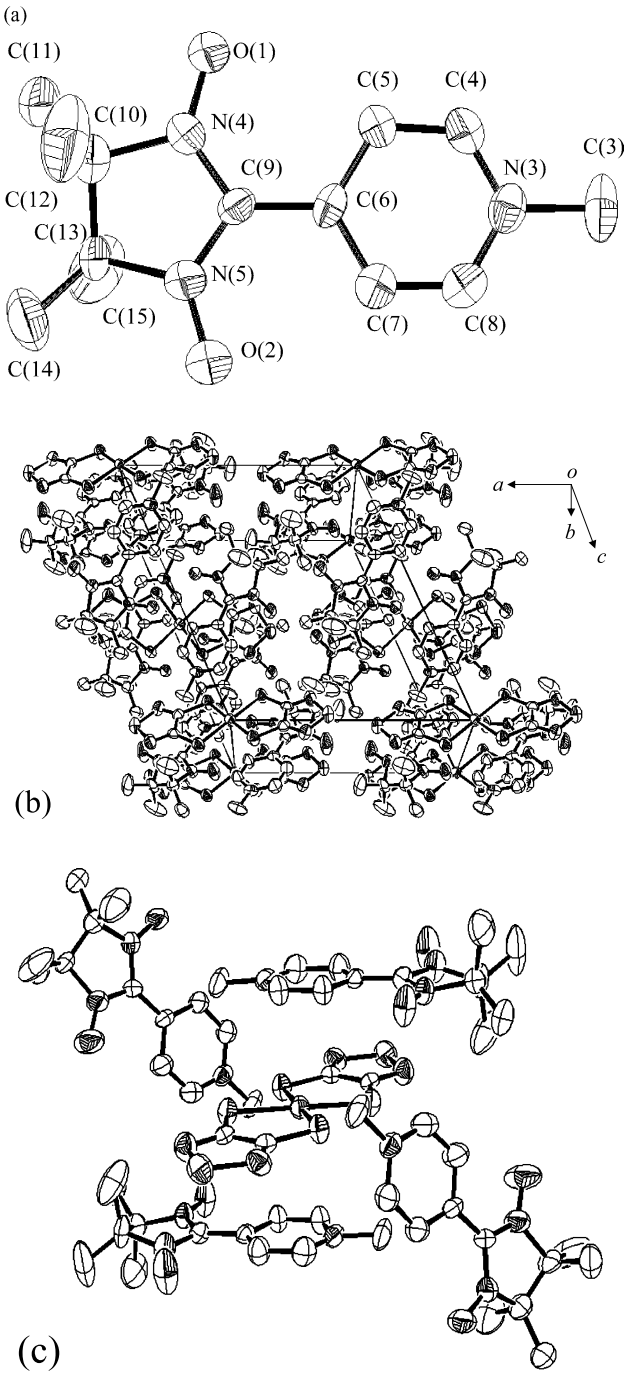

Fig. 4. The molecular and crystal structures of $(p\text{-MPYNN})_2Ni(tdas)_2$ (a) the m-MPYNN cation; (b) the unit cell; (c) the crystal packing around the $Ni(tdas)_2$ anion.

sulfur atoms is 3.52 Å, which is shorter than the sum of the van der Waals radii of sulfur atoms. The p-MPYNN cation is present as a centrosymmetric dimer. The shortest contact within the dimer is 3.35 Å, which is observed at the oxygen atom of the NO group, O(1). Intermolecular contact is also observed between p-MPYNN and $Ni(tdas)_2$. The $Ni(tdas)_2$ anion is surrounded by four p-MPYNN molecules, two of which are close to both sides of the anion. The others are in close proximity to the anion from the upside and downside. The pyridyl ring stacks face to face with the five-membered ring containing the Ni atom. The distances between the rings are within 3.6 Å, and the shortest contact is 3.42 Å between Ni(1) and C(4). Contact between the NO group and $Ni(tdas)_2$ is not recognized.

3.3. Physical properties of (m- or p-MPYNN)$_2$Ni(tdas)$_2$

Fig. 5 shows the temperature dependence of the paramagnetic susceptibilities, χ_p, of (m- and p-MPYNN)$_2$Ni(tdas)$_2$, where χ_pT is plotted as a function of temperature. The χ_pT values of (m- and p-MPYNN)$_2$Ni(tdas)$_2$ decrease with decreasing temperature, indicating antiferromagnetic intermolecular interactions.

The magnetic behavior of (m-MPYNN)$_2$Ni(tdas)$_2$ is well interpreted in terms of the modified singlet–triplet model [3],

$$\chi_p = \frac{4C}{T[3 + \exp(-2J/k_BT)] - \theta} \quad (1)$$

where J is the intradimer coupling constant, θ is the Weiss constant, C is the Curie constant and k_B is the Boltzmann constant. The solid curve fitted to the plots for (m-MPYNN)$_2$Ni(tdas)$_2$ in Fig. 5 is the theoretical best fit of Eq. (1) with the parameters, $J/k_B = -3.3$ K, $\theta = -6.4$ K and $C = 0.736$ emu K mol^{-1}. The intradimer interaction was suggested to be antiferromagnetic, although the relative orientation of the m-MPYNNs usually displayed a ferromagnetic interaction. This is presumably because the dihedral angle between the rings is small.

The magnetic behavior of (p-MPYNN)$_2$Ni(tdas)$_2$ can be understood with the Curie–Weiss law (Eq. (2)). The

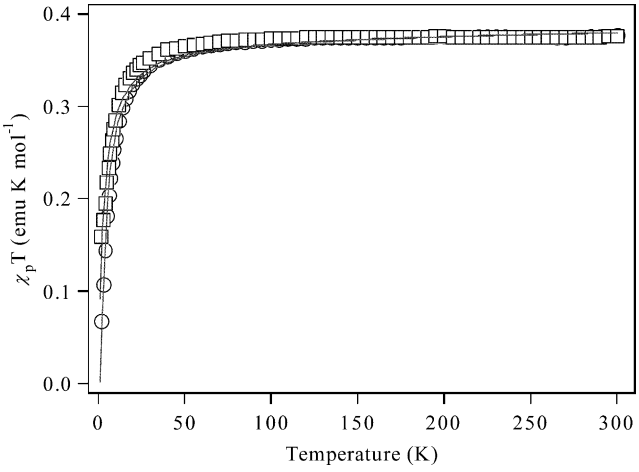

Fig. 5. Temperature dependence of the paramagnetic susceptibilities of the (m-MPYNN)$_2$Ni(tdas)$_2$ complex (circles) and (p-MPYNN)$_2$Ni(tdas)$_2$ complex (squares). The solid curves are theoretical ones. See the text.

best fit curve in Fig. 5 is obtained with the Curie and Weiss constant of $C = 0.376$ emu K mol^{-1} and $\theta = -3.1$ K, respectively.

$$\chi_p = \frac{C}{T - \theta} \quad (2)$$

The χ_p value of (p-MPYNN)$_2$Ni(tdas)$_2$ dose not show a maximum even at low temperature. Therefore, the magnetic behavior of (p-MPYNN)$_2$Ni(tdas)$_2$ cannot be fitted by the dimer model, although p-MPYNNs exist as a dimer.

In addition, both complexes did not show good electrical conductivity, and they were classified as insulators.

4. Conclusion

We have prepared two novel Ni(tdas)$_2$ complexes, (m-MPYNN)$_2$Ni(tdas)$_2$ and (p-MPYNN)$_2$Ni(tdas)$_2$. The magnetic interaction between the radicals was antiferromagnetic in both complexes. Hybridization between the paramagnetic complexes and organic cation radicals is in progress.

5. Supplementary data

Supplementary data are available, upon request, from the CCDC, 12 Union Road, Cambridge CB2 1EZ, UK, quoting the deposition numbers 194518 and 194519.

Acknowledgements

This work is partially supported by grants from the Ministry of Education, Culture, Sports, Science and Technology, Japan (No. 12740380 and 14740385).

References

[1] H. Kobayashi, A. Kobayashi, P. Cassoux, Chem. Soc. Rev. 29 (2000) 325.
[2] K. Awaga, A. Yamaguchi, T. Okuno, T. Inabe, T. Nakamura, M. Matsumoto, Y. Maruyama, J. Mater. Chem. 4 (1994) 1377.
[3] K. Awaga, T. Okuno, A. Yamaguchi, M. Hasegawa, T. Inabe, Y. Maruyama, N. Wada, Phys. Rev. B 49 (1994) 3975.
[4] A. Yamaguchi, T. Okuno, K. Awaga, Bull. Chem. Soc. Jpn. 69 (1996) 875.
[5] H. Imai, T. Inabe, T. Otsuka, T. Okuno, K. Awaga, Phys. Rev. B 54 (1996) 6838.
[6] I. Hawkins, A.E. Underhill, J. Chem. Soc., Chem. Commun. (1990) 1593.
[7] O.A. Dyachenko, S.V. Konovalikhin, A.I. Kotov, G.V. Shilov, E.B. Yagubski, C. Faulmann, P. Cassoux, J. Chem. Soc., Chem. Commun. (1993) 508.
[8] S. Shenk, I. Hawkins, S.B. Wilkes, A.E. Underhill, A. Kobayashi, J. Chem. Soc., Chem. Commun. (1993) 1648.
[9] N. Robertson, K. Awaga, S. Person, A. Kobayashi, A.E. Underhill, Adv. Mater. Opt. Electron. 8 (1998) 93.
[10] H. Yamochi, N. Sogoshi, Y. Simizu, G. Saito, K. Matsumoto, J. Mat. Chem. 11 (2001) 2216.
[11] K. Awaga, T. Okuno, Y. Maruyama, A. Kobayashi, H. Kobayashi, S. Schenk, A.E. Underhill, Inorg. Chem. 33 (1994) 5598.